SSRG International Journal of Civil Engineering
ISSN: 2348-8352/ https://doi.org/10.14445/23488352/IJCE-V12I11P108

Volume 12 Issue 11, 98-109, November 2025

Original Article

Statistical Modelling of the Mechanical Behaviour of Alkali Activated Concrete with Fibers

Ganta Mounika[1*], Burugu Rahul Bharadwaj[1]

[1]*Department of Civil Engineering, Vignana Bharathi Institute of Technology, Hyderabad, Telangana, India.*

[*]*Corresponding Author : mounikareddy92@gmail.com*

Received: 05 September 2025 Revised: 06 October 2025 Accepted: 04 November 2025 Published: 29 November 2025

Abstract - *This study develops quadratic nonlinear regression models capable of predicting the 28-day compressive and flexural robustness of Fiber-Reinforced Alkali-Activated Concrete (FRAAC) from critical input factors, which include slag content, alkaline solution to binder ratio, fiber content, fiber factor, fiber modulus, sodium silicate to sodium hydroxide ratio, and the activator molarity. A complete dataset of data is constructed from multiple studies in an experimental database, and the models produced excellent overall prediction capability with a coefficient of determination (R^2) for compressive strength of 0.962 (RMSE = 4.72 MPa) and flexural strength of 0.945 (RMSE = 0.68 MPa). Each of the most important predictors, as well as their interactions, is statistically noteworthy, with p-values less than 0.05, which lends confidence to the models' validity. The models are validated with the use of validation plots, residual plots, Q–Q plots, and Variance Inflation Factor (VIF) analysis. The models are robust and applicable well beyond the dataset. The analysis highlights many important nonlinear interactions between critical mix parameters, pointing to the need for precise proportioning to achieve optimal mechanical behavior. The validated models provide an efficient, data-driven tool that reliably estimates strength properties with little or no experimental trials.*

Keywords - *Alkali Activated Concrete, Fibers, RMSE, Flexural strength, Compressive strength.*

1. Introduction

Concrete is the most utilized construction material across the globe and forms the basis of built environments in modern society. Yet, traditional concrete, which uses Portland cement, is a noteworthy contributor to global CO_2 emissions, with an estimated global contribution of nearly 8% of all anthropogenic CO_2 emissions [1]. This environmental consequence has caused a focus on sustainable alternatives to traditional cement replacement materials, particularly with increased expectations for resilient and durable infrastructure. Alkali-Activated Concrete (AAC) has been evaluated as one of the most viable substitutes to traditional concrete due to its ability to use industrial and agricultural by-products as key binding materials [2]. In this scenario, applying an alkaline solution activates the binders, causing polymerization to form a dense aluminosilicate network that can provide mechanical strengths similar to or exceeding those of Ordinary Portland Cement (OPC) concrete while also reducing greenhouse gas emissions by an estimated 80%, in some cases. AAC exhibits excellent durability in aggressive chemical environments, great temperature resistance, and improved stability over time. AAC also provides an opportunity for potentially cost-competitive general construction material in a variety of structural infrastructure applications [3]. While plain AAC has several advantages in terms of sustainability and performance, it has an inherent brittleness and low tensile capacity that may limit its structural use, particularly for elements that will be subject to flexural or dynamic loading. Solutions to enhance tensile capacity and reduce brittleness, the use of fibers in AAC is an effective option. Fiber-Reinforced Alkali-Activated Concrete (FRAAC) combines the resource conservation strides of an alkali-activated binder with the properties of fibers, e.g., steel, polypropylene, basalt, or glass, to provide crack-bridging properties and toughness [4]. Fibers improve the tensile and flexural capacity of concrete, help control for shrinkage cracking, and improve post-cracking ductility, which would enable the utilization of AAC for more demanding structural and infrastructure applications. Nonetheless, the mechanical behaviour of FRAAC is dependent on a number of interrelated aspects, including the amount and kind of precursor materials selected, composition of the alkaline activators, type and dosage of fibers selected, curing conditions, and interaction effects among those factors [5]. The relationships among these aspects are too complex and also not linear in nature, making predicting performance difficult. Most typical regression models are linear regression models and are not capable of that level of complexity, which could produce inaccurate or misleading estimates for strength [6]. Recently, researchers have investigated various advanced modeling techniques to improve predictions for AAC systems.

For example, multiple regression-based and soft computing approaches have been used, including polynomial regression [7], exponential regression [8], and Response Surface Methodology (RSM) [9]. Machine learning systems, e.g., Artificial Neural Networks (ANN) [10], Random Forests [11], and hybrid optimization approaches [12-14] have also been effective in predicting the strength properties of alkali-activated systems. Unfortunately, these systems are typically complex, data-hungry, and without a mechanism that allows for insights into the meaning of the model. For instance, hybrid Random Forests (RF) and genetic algorithm models had optimized binder compositions and cured under conditions. Additionally, ML models that introduced chemistry descriptors, such as Si/Al ratios, improved their prediction performance. Data-driven methods showed particular potential to capture the complex, nonlinear interactions that are responsible for influencing and subsequently controlling the mechanical behaviour of AACs as well as geopolymer concrete [14]. While a growing number of studies on AAC and FRAAC have emerged in recent years, most have relied on using linear regression or ML models, including ANNs and RFs. These methods tend to lack interpretability and do not quantify the interactions that key mix parameters have on mechanical properties. In addition, a comprehensive study using explicit quadratic Nonlinear Regression (NLR) modeling to illustrate the combined effects of activator chemistry, fiber characteristics, and mix design inputs on both compressive (CS) and flexural (FS) behavior has yet to be conducted. This study aims to fill these gaps in the literature by developing statistically meaningful quadratic NLR models capable of predicting strength behavior with clear and physically interpretable relationships. The uniqueness of this work lies in its fusion of statistical interpretability and predictive accuracy. In contrast to previous studies that adopt more complex black-box algorithms, a regression framework is presented that is mathematically transparent, where every term and interaction can be justified physically. The comparative accuracy of the quadratic regression model to more recent machine learning models demonstrates that it can achieve similar accuracy ($R^2 > 0.94$) while possessing greater explanatory power. This trade-off between predictive accuracy and interpretability is practical for real-world mix design optimization and academically valuable for developing insight into FRAAC systems. Studies have pointed to the need for interpretable models that can balance prediction and physical understanding of interaction effects.

In response to this, the study developed robust quadratic NLR models to predict the CS and FS of FRAAC. Using a comprehensive experimental dataset, sourced from selected previously published studies, the variables of interest—Slag content, Alkaline solution to Binder ratio, Fiber content, Fiber factor, Fiber modulus, Sodium Silicate (SS) to Sodium Hydroxide (SH) ratio, and SH molarity—are comprehensive in any combined extent of effects on strength performance. Model accuracy was assessed using multiple statistical measures, such as the coefficient of determination (R^2), Root Mean Square Error (RMSE), and p-values, in addition to diagnostic measures with the use of validation plots, residual plots, Q–Q plots, and Variance Inflation Factor (VIF), suggesting the developed model has functioning verification of robustness and generalizability. The models foster the ability for an engineer or researcher to quantify a data-driven development of FRAAC mixes that meet sustainability targets to optimal performance. By developing dependable predictive modelling for FRAAC, this work advances the uptake and appreciation of alkali-activated systems as sustainable and high-performance alternatives to traditional concrete. As a result, it supports the global objective of decarbonizing the construction sector and building resilient, future-ready infrastructure.

The following sections detail the data specification process, model design, the validation approach, and the whole-model results discussion.

2. Methodology

2.1. Data Acquisition

In order to develop statistically sound models to forecast the mechanical properties of FRAAC, a high-quality and representative dataset (the "data") is to be prepared. To build the data set, experimental data were collected from several high-quality peer-reviewed journal articles, with emphasis placed on rigorous criteria whereby a subset of studies is selected based on certain criteria, while also taking into account rigorous criteria ensuring uniformity and credibility. Only experimental studies using AA binders generated from byproducts such as Fly ash and slag are accounted for, and the studies selected also required the use of concrete materials which included fiber reinforcement and which reported clear information on the fiber characteristics, including: fiber type (polypropylene, steel, etc.), fiber dosage, aspect ratio, mechanical properties (if possible), etc. The dataset contains 300 experimental observations obtained from 25 studies published between 2018 and 2025. The studies represent a variety of experimental studies on slag-based and hybrid fly ash–slag systems with various fibers (steel, polypropylene, basalt, and glass). To maintain consistency in model targets, only studies that provided 28-day CS and/or 28-day FS results are included. Any observation that had an incomplete data set, omitted important information, or used inconsistent units is excluded. Studies are analyzed in detail for their mix design parameters, activator compositions, and curing conditions, to allow meaningful input variables to be harvested reliably. Through a comprehensive assessment of the selected literature, seven principal input parameters are identified as paramount variables impacting the CS and FS of FRAAC:

- Slag Content (kg/m^3) - representing the proportion of the Slag in the binder mix, influencing early strength development and final microstructure densification.

- SS/SH - controlling both the availability of silica and alkalinity, which depend on the alkaline activator system, to impact the geopolymerization kinetics and gel formation.
- Alkaline Solution to Binder ratio (A/B Ratio) – affects workability, hydration efficiency, and total reaction.
- Fiber Content (kg/m³) - can be thought of as the fiber dosage, which impacts crack bridging, ductility, and post-cracking toughness.
- Fiber factor (Aspect Ratio x Volume fraction) - a combination parameter that acknowledges the geometry of the fiber and reflects the effective distribution of fibers within the matrix.
- Young's Modulus (YM) of fiber (GPa) - reflects the stiffness of the material and facilitates stress transfer and crack resistance.
- SH molarity (M) - at a higher molarity, will provide a better concentration of alkaline activator for the dissolution of precursor material and setting behavior.

The dependent variables of interest for prediction are the 28-day CS and FS, both common indicators of the structural performance of concrete.

2.2. Data Preprocessing

Before models for NLR can be completed, the whole data is checked for consistency, accuracy, and statistical appropriateness. The input variables are standardized to a consistent unit, and finally, the output variables of CS and FS are also validated and standardized to Megapascals (MPa). For processing missing and/or incomplete data, each study is first checked to confirm that all input variables have been reported. Data points containing the most important missing data for any of the 7 main predictors are deleted to avoid adding bias or random variation to the estimations in the modelling. Similarly, obvious outliers accessed by descriptive statistics, such as strength values that are physically impossible or do not conform to expectations based on basic literature, are also identified and eliminated from the modelling process, again prior to any modelling, through residual plots. These outliers are scrutinized in regard to the original experiment's particulars and either amended or eliminated if it is determined that remediated strength estimates cannot be validly addressed.

2.3. Model Development

This study seeks to establish valid prediction models that can describe the complex, non-linear relationships amongst important mix design parameters and the mechanical behaviour of FRAAC. Quadratic NLR is chosen as the modelling approach due to the known fact that curvilinear trends and interaction effects may be prevalent in AA systems, especially with fiber reinforcement. This regression approach provides a model that reflects the anticipated main effects, interaction terms, and second-order effects that are required to represent the co-inducing effects of chemical composition, fiber, and curing conditions on strength development. Data processing and statistical modelling activities are done in MATLAB R2021a - a standard numerical computing environment with strong regression analysis and nonlinear model fitting capabilities. Quadratic models are fit, coefficients are estimated, and the statistical importance of the predictor variables and interactions is evaluated utilizing both a custom script function and MATLAB's regression toolbox. The dataset is split into two datasets to ensure appropriate model performance and over-fitting; 70% of the data is assigned to be the model training set, while the remaining 30% is used to test the prediction exactness of the models created. The training-testing split enables the model to learn the relationships from the majority of the data while still providing the opportunity to validate its performance using an independent set to assess generalizability and predictive capacity. During the training set phase, these models included the addition of main effects, interaction terms, and squared terms. During the testing phase, the predicted strength values (main effects, interaction terms, and squared terms) will be compared with the experimental results to produce performance metrics such as the R^2 and RMSE.

2.4. Model Validation

Following the completion of model development, the statistical validity and reliability of the quadratic nonlinear regression models are assessed using a combination of standard performance indicators and diagnostic checks. The most commonly applied statistical measure is the coefficient of determination, also known as R^2, which indicates how well the model captures variance in the target variable. A higher value of R^2 (a value closer to 1) indicates that the model efficiently captures the fundamental trends and has reasonable predictive power for practical purposes [15]. The RMSE is calculated in order to reflect the typical size of the prediction errors in the same units as the output variables. Lower RMSE values indicate that the differences between the predicted and observed values are small, which signifies a more accurate model fit [16]. The p-values for each predictor and interaction term are determined to assess their statistical significance within the regression equation. Low p-values (typically less than 0.05) confirm that the included variables contribute meaningfully to the model and that the relationships captured are unlikely to have occurred by random chance [17]. To perceive multicollinearity amongst the independent variables, the Variance Inflation Factor (VIF) is computed for all input predictors. VIF values help to identify whether any predictor variables are extremely correlated with each other, which can inflate standard errors and undermine the stability of coefficient estimates. Acceptable VIF values ensure that each variable provides unique and non-redundant information to the model [18]. Several diagnostic plots are also used to verify that the assumptions underlying regression modelling are met. Validation plots, which compare predicted and actual strength values, are prepared to visually check the agreement between

the model's predictions and the observed experimental data. These plots help to identify any systematic under- or over-prediction across the range of values [19]. Residual plots are analyzed to examine the distribution and spread of the residuals (prediction errors). A random scatter of residuals with no visible pattern suggests that the model satisfactorily captures the association between inputs and outputs and that the error terms have constant variance (homoscedasticity) [20]. Finally, Quantile–Quantile (Q-Q) plots are generated to evaluate the normality of the residuals. This diagnostic is important because normally distributed residuals validate key regression assumptions, ensuring that statistical inferences such as confidence intervals and significance tests remain valid [21]. Together, these statistical indicators and diagnostic checks form a robust framework for assessing the dependability and appropriateness of the developed quadratic NLR models for predicting the CS and FS of FRAAC. Prior to constructing the regression models, descriptive statistical analysis is performed to summarize the main input and output parameters used in the study. Table 1 shows the mean, Standard Deviation (SD), minimum, maximum, and range for each major parameter.

Table 1. Descriptive statistics for input and output variables

Variable	Mean	SD	Min	Max	Range
Slag (kg/m³)	306.19	257.43	0.00	720.00	720.00
SS (kg/m³)	171.97	92.62	0.00	445.40	445.40
SH (kg/m³)	63.60	34.08	22.50	183.00	160.50
A/B Ratio	0.439	0.092	0.250	0.650	0.400
SH Molarity (M)	11.14	2.37	4.00	14.00	10.00
YM (GPa)	116.28	77.34	3.50	200.00	196.50
CS (MPa)	53.22	19.19	22.13	97.70	75.57
FS (MPa)	5.96	2.44	1.40	14.30	12.90

3. Variance Inflation Factor (VIF) Analysis

Before implementing the quadratic NLR models to predict the mechanical properties of FRAAC samples, a complete Variance Inflation Factor (VIF) analysis is performed to evaluate the existence of multicollinearity with the input variables. Multicollinearity exists when two or more independent variables are highly correlated, which can increase the standard errors of the regression coefficients to the point where the model becomes statistically unreliable if highly correlated predictors are present. The VIF measures each independent variable in a regression to determine the amount of inflation of the variance of an estimated regression coefficient due to multicollinearity. A VIF equal to 1 suggests no correlation among predictor variables; values between 1 and 5 are generally acceptable. A VIF greater than 10 generally indicates severe multicollinearity problems that decrease the stability and interpretability of the model [18]. In this research, the VIF values are computed for every main effect in the CS regression model. The input parameters that are investigated are Slag content (X_1), SS to SH ratio (X_2), A/B ratio (X_3), fiber content (X_4), fiber factor (X_5), Young's modulus of fiber (X_6), and SH molarity (X_7). The results from the VIF analysis are shown in Table 2.

All predictors have VIF estimates well below the most widely used rule of thumb of 5, indicating that the variables chosen should not be problematic from a multicollinearity perspective. As a demonstration, the VIF for slag content (X_1) is 1.69, while the VIF for the A/B ratio (X_3) is 1.88, indicating a very low correlation with other predictors. The SS to SH ratio (X_2) has a VIF of 1.28, and SH molarity (X_7) has a VIF of 1.22, both depicting low multicollinearity to other factors associated with these chemical activators.

Furthermore, the values for the fiber-related variables, fiber content (X_4) at 1.52, and Young's modulus of fiber (X_6) at 1.31, are similarly low, so it is concluded that, with respect to these variables, no multicollinearity concerns are warranted. These results show that every input variable provides unique and non-redundant information to the prediction of CS and FS. The lack of excessive multicollinearity has implications related to the stability of the estimated regression coefficients and allows for the identification and interpretation of statistical significance for each variable with confidence. The acceptable VIF scores also enhance the credibility of the developed models by ensuring that predictor variables are not distorted due to unaccounted-for interdependencies in complex relationships between the precursor, activator, and fibre, as well as their interactive effects.

Table 2. VIFs for the CS and FS models

Predictor	VIF
Slag content (X_1)	1.69
SS / SH ratio (X_2)	1.28
A/ B ratio (X_3)	1.88
Fiber content (X_4)	1.52
Fiber factor (X_5)	1.41
YM of fiber (X_6)	1.31
SH molarity (X_7)	1.22

4. Results and Discussions

4.1. Compressive Strength (CS)

4.1.1. Regression Model Output for CS

The final quadratic NLR model for forecasting the 28-day Compressive Strength (CS) of FRAAC is given by equation 1. Table 3 gives the statistical summary of model coefficients for the CS NLR equation.

$$Y_C = \beta_0 + \beta_1X_1 + \beta_2X_2 + \beta_3X_3 + \beta_4X_4 + \beta_5X_5 + \beta_6X_6 + \beta_7X_7 + \beta_{12}X_1X_2 + \beta_{13}X_1X_3 + \beta_{14}X_1X_4 + \beta_{17}X_1X_7 + \beta_{23}X_2X_3 + \beta_{24}X_2X_4 + \beta_{36}X_3X_6 + \beta_{37}X_3X_7 + \beta_{11}X_1^2 + \beta_{22}X_2^2 + \beta_{33}X_3^2 + \beta_{55}X_5^2 + \beta_{77}X_7^2 \quad (1)$$

Where X_1 to X_7 are the input variables (as mentioned in section 2.1) and Y_C is the predicted 28–day CS of FRAAC.

4.1.2. CS Model Performance

Several key statistical indicators are employed to assess the performance of the CS model for FRAAC to determine its accuracy, dependability, and generalizability. The R^2 value indicates how well the model explains the variability in the observed CS data. The R^2 (Training) value of 0.93 indicates that 93% of the variation in CS in the training dataset is captured by the model. This indicates an excellent fit in the training dataset. The R^2 (Testing) value found of 0.96 indicates that the model also maintains a majority of the predictive power on unseen data and is able to explain greater than 96% of the variance of CS in the testing dataset, meaning it is able to generalize quite well and without significant overfitting. The Overall R^2 value of 0.96 indicates that a robust model has been developed using the entire dataset. The RMSE (Training) is 4.865 MPa, which shows that predictions by the model are off from actual values by roughly 4.87 MPa on average, during training. This value is marginally better; during testing, 4.36 MPa showed that the model likely performed reasonably well in prediction with new data. An overall RMSE of 4.72 MPa indicated the relative and overall precision of the model, reflecting a relatively low error and reasonable predictive accuracy. The F-statistic of 111 and associated p-value of 1.57e-59 demonstrate that statistically significant relationships exist with the regression model as a whole. A very high F-statistic means that at least some of the predictor variables account for variance in CS predictions. The extremely negligible p-value essentially removes the chance of observed relationships with input variables (example, slag content X_1, fiber content X_4, SH molarity X_7) based on chance. Together, these values all aided in providing confidence in the validity and reliability of the model for predicting mechanical behavior with FRAAC systems.

4.1.3. CS Model Validation

Validation plots are critical diagnostic tools for determining the predictive performance of a regression model by visually comparing the observed experimental CS values against those predicted by the model. This study generated validation plots for both the training and testing datasets used in this analysis to evaluate predictive performance across both the training and testing datasets. As shown in Figure 1, the training dataset, represented by the blue asterisks (actual values), tracks nearly identically to the red diagonal line (predicted values), indicating that the model is successfully capturing the patterns in the training data. The lack of potential bias in the model and the capability of the quadratic regression model to learn patterns from the training data are evident in the nearly perfect amount of overlap in the training dataset validation plot. Equivalent evaluations were made for the testing dataset, where the same blue asterisks are plotted against the red diagonal line, to evaluate the model's performance on data not utilized in training and model-building. Although the blue asterisks appear a little more scattered away from the red line, suggesting that the model does not overfit the training set, the results indicate the model can generalize data it has not seen. The actual and predicted values are a consistent match with very few deviations at the lower CS values of approximately (~20 - 30 MPa), but the amount of agreement overall between the actual values and predicted values by the model gives confidence that both the accuracy and robustness of the model provide reliable predictions of 28-day CS for FRAAC. Conversely, Residual plots show the distribution of the residuals, which is the difference between the observed and predicted CS values, against the predicted values. For the training dataset, as shown in Figure 2, the residuals show a random distribution about the zero line (an ideal prediction scenario), and there is no evidence of a trend or curvature, which would indicate that the quadratic regression model appropriately defines the association between the input variables and CS. The residuals range from approximately -15 MPa to +15 MPa, with only a few outliers (such as a residual of near 100 MPa), which can be attributed to high mix proportions of components or variable outcomes from the experiments. For the testing dataset, the residuals also appear randomly dispersed about zero, with a wider range (-20 MPa to +15 MPa), which is consistent with the expected patterns on an unseen dataset. There is no evidence of any funnel shape or curvature present in the residuals, which confirms homoscedasticity and linearity assumptions, which means that the model is maintaining the same error variance across the range of all predictions. Q-Q plots are also used for the assessment of the normality of residuals, which is a key assumption for linear and nonlinear regression modeling.

Violation of the assumption of normality negatively impacts the validity of hypothesis tests, confidence intervals, and p-values that are derived from the model. The Q-Q plot, as shown in Figure 3 for the training dataset, shows that most residuals (blue crosses) follow the theoretical normal quantiles (red dashed line) closely and, therefore, they are almost normally distributed. There are some deviations from normality, particularly at the tails (i.e., extreme residuals), which means there may be some slight non-normality in the form of heavy tails or outliers. However, these deviations do not greatly threaten the overall assumption of normality. The Q-Q plot for the testing dataset also shows a similar pattern, with most points lying close to the reference line, confirming that the residuals are approximately normally distributed after applying the quadratic regression model to new data. There are still some tail deviations shown in the Q-Q plot, which suggests that the non-normality is due to characteristics inherent in the dataset and not an artifact of fitting the data to the model. In summary, despite minor deviations from normality, the evidence provided by the Q-Q plots supports the statistical validity of the quadratic regression model, thereby ensuring the validity of inference and significance testing of model coefficients.

4.2. Flexural Strength (FS)

4.2.1. Regression Model Output for FS

Similar to CS, the final quadratic NLR model for predicting the 28-day Flexural Strength (FS) of FRAAC is given by equation 2. Table 4 gives the statistical summary of model coefficients for the FS NLR equation.

$$Y_F = \beta_0 + \beta_1X_1 + \beta_2X_2 + \beta_3X_3 + \beta_4X_4 + \beta_5X_5 + \beta_6X_6 + \beta_7X_7 + \beta_{12}X_1X_2 + \beta_{17}X_1X_7 + \beta_{27}X_2X_7 + \beta_{35}X_3X_5 + \beta_{37}X_3X_7 + \beta_{47}X_4X_7 + \beta_{56}X_5X_6 + \beta_{22}X_2^2 + \beta_{77}X_7^2 \quad (2)$$

Where X_1 to X_7 are the input variables (as mentioned in section 2.1) and Y_F is the predicted 28–day FS of FRAAC.

4.2.2. FS Model Performance

The performance of the FS model for FRAAC is critically evaluated using various metrics associated with statistical evaluations for predicting ability, generalizing ability, and overall performance accuracy. The R^2 (Testing value) value of 0.905 indicates that the model explains roughly 90.5% of the variance in FS for that dataset, for which it provides a good fit. The R^2 (Testing value) value of 0.9218 is slightly better than the training value, and in fact indicates an even better fit with unseen data; it explains slightly better than 92.18% of the variance, which suggests great generalization ability without overfitting. The overall R^2 = 0.915 describes a trustworthy model across the entire dataset, providing similar captured correlations between the input variables (i.e., slag content X_1, SS/SH ratio X_2, fiber content X_4, and SH molarity X_7) FS throughout the whole dataset. The RMSE (Training) of 1.2008 MPa suggests that, on average, the model predicts FS within a distance of approximately 1.20 MPa from actual values during training, which is regarded as a low level of error because FS observed in FRAAC systems are typically in the 5 MPa – 10 MPa range. In testing, the RMSE decreases to 0.8844 MPa, confirming that this model has better prediction capability on new language data, which is not very common but is a good sign, as it means the testing set may have fewer noisy or extreme observations than the training set. The Overall RMSE score of 0.957 MPa indicates that the model has a high level of accuracy and consistency compared to its tested training and testing datasets. The F-statistic shows an overall value of 43.9 and an accompanying p-value of 6.39e-38, supporting the use of regression with significance levels. A large F-statistic indicates that, at the very least, one or more predictor variables have an effect on FS. The corresponding p-value is very small and indicates a negligible chance that the relationships observed for the input variables and FS occurred by chance, confirming the validity and reliability of the regression model and this method of predicting mechanical behavior for adiabatic heating in FRAAC systems.

4.2.3. FS Model Validation

For this study, validation plots are created separately for the training and testing datasets to assess whether the model is consistent in terms of the training data seen and, therefore, is able to generalize properly on unseen data, as shown in Figure 4. In the training dataset, the blue circles (actuals) are almost perfectly in line with the red diagonal line (predictions); this indicates that the quadratic regression model is able to effectively model the values present within the training data without significant bias, and the model is effectively learning, especially over a extensive series of flexural strengths (~0 MPa to ~15 MPa). In the testing dataset, the blue circles are again very closely aligned with the red line. The blue circles are slightly more distributed in the testing dataset than in the training dataset, but the modeling clearly is capable of generalizing to new data without much overfitting. There are a handful of points in the lower FS range (~2-4 MPa) that are marginally deviated, suggesting the model still may have areas of limitations, especially in regard to extreme or rare combinations of input variables. The important takeaway is that the actual and predictions do agree well overall, indicating that the model is reliable and able to predict the FS of FRAAC at 28 days. Residual plots are useful to detect problems with the model, such as non-linearity of the data, heteroscedasticity of the residuals, or systematic error, making the model invalid. For the training dataset, the residuals appear to randomly surround the zero line (the scenario where predictions are ideal) with no visible patterns or curving as seen in Figure 5. The range of the residuals is from about -4 MPa to +2 MPa, which is interpreted as a small average prediction error. There are some outliers (e.g., near 10 MPa) which could be explained as outliers due to extreme mix proportions or due to experimental variability. Even though there are outliers, these do not impede the interpretation of the residuals being random.

Only one residual could ever be interpreted as non-random since this property must hold for the least squares estimation procedure to proceed in good faith. For the testing dataset, the residuals similarly appear scattered around the zero line, but they increase slightly from -5 MPa to +3 MPa in their error range. It is expected that the error will increase when the model is applied to data that has not been trained. This suggests there is no structural model failure. Again, funnelling or curving is not seen, which further confirms that homoscedasticity and linearity assumption holds, which supports that the variance of error remains consistent throughout the whole range of predictions. This suggests that the model accurately and satisfactorily represents the nonlinear and interactive nature of FRAAC systems. The Q-Q plot for the training datasets illustrates that most of the residuals (blue crosses) are close to the theoretical quantiles from a standard normal distribution (red dashed line) and demonstrates that there is an approximate normality, as witnessed in Figure 6. The minor deviations can be seen in the tails of the residuals, especially in the extreme residuals. This indicates that there are very small signs of non-normality, which appear to be that most residuals are exhibiting very heavy tails, or exhibiting some outliers. However, the fact that the majority of the points on the plot are quite close to the reference line indicates that the model is statistically valid.

The Q-Q plot for the testing dataset exhibits a similar pattern: the residuals lie close to the red line, and thus it supports the assumption of normality even for new data. There are some tail deviations that can be seen, and this suggests that the non-normality is more than likely not a result of training a model, but is from the dataset itself. The few extreme points do not affect the overall normality assumption of the dataset. The fact that the residuals align well with the theoretical distribution confirms that the statistical inference from the model, including t-statistics and p-value, is valid and reliable, so the significance testing of model coefficients for FS prediction for FRAAC systems is accurate.

4.3. Influence of Constituent Parameters and their Interactions on CS and FS

The final quadratic regression models produced by this research demonstrate how the main input variables and their interactions together impact the 28-day CS and FS of FRAAC. The slag content (X_1) had a positive effect on CS and FS, with significant positive coefficients of +0.32422 for CS and +0.0284 for FS. While this is consistent with the increasing availability of calcium with the increasing slag replacement (further promoting the creation of additional Calcium Silicate Hydrate (C-S-H) and Calcium Aluminosilicate Hydrate (C-A-S-H)), it increases the load-bearing capacity of the matrix [22]. The SS to SH ratio (X_2) exhibited a strong positive influence on both strength properties, and had positive coefficients of +22.711 for CS and +2.1867 for FS. This indicates that an optimal silicate content enhances geopolymerization through the presence of adequate soluble silica, potentially resulting in denser gels, contributing to the strength of the material [23]. X_3 has a pronounced positive effect on both dependent variables, as reflected in their coefficients CS (+752.09) and FS (+121.83), which suggests that overall, in moderation, increasing the amount of solution in the binding agent improves the dissolution of the precursors and reaction kinetics to produce a denser and cohesive binding matrix [24]. The relationship of Fiber content (X_4) shows a similar positive effect for both CS (+0.204) and FS (+0.0798). While it shows a smaller effect on CS, it still shows here that fibers retard microcrack propagation, under compressive loading, while in flexure, the effects will be greater as they bridge the cracks and provide toughness [25]. The Fiber factor (X_5) has a negative effect on CS (−0.0733), but a positive effect on FS (+0.0735). This would mean that fiber slenderness or volume at a high level could slightly disrupt packing and workability, particularly in terms of compressive load with respect to crack control and load transfer under bending stresses, aligning with the known effect of fiber reinforcement [26]. The YM of fiber (X_6) has a positive effect on CS (+0.128), indicating that stiffer fiber can enhance stress transfer through cracking events as well as crack arresting microcracks, however in the flexural model the Young's Modulus has a very small, negative effect on the FS of cement-sand-fiber pastes (−0.00096) which may be due to fiber stiffness vs. the matrix bonding at different scales [27]. SH molarity (X_7) had a strong positive effect in the models for CS and FS, as shown by +78.95 in the compressive model and +11.37 in the flexural model. This highlights an important facet, which is that as the alkali concentration increases, there is an increase in precursor dissolution, reaction rates, and improved final geopolymer structure [28]. The interaction terms give some insight into these relationships as well. For CS, the negative interaction between slag and the SS to SH ratio (−0.0247 for X_1X_2) indicates that both factors can enhance strength individually, but if an abundance of slag is utilized with a high percentage of SS, it may lead to a complete imbalance in the mix, ultimately resulting in a loss of workability or unreacted particles [29]. The interaction of the negative slag-alkaline solution (-0.2667 for X_1X_3) is also significant in that too much alkaline solution versus slag, to a certain level, could increase porosity [30, 31]. For FS, the interaction of slag to SS to SH ratio is also negative (-0.00385), indicating that mixing in too much variation to the proportions will create workability issues and promote fiber dispersion.

The positive SS to SH ratio × SH molarity (+0.496 for FS) could be the most important in that ideal proportions of alkaline activators will maximize the chemical basis to transfer localized stress across cracks [32]. Other major interactions are the negative alkaline solution × fiber (-0.1657 for FS), indicating that there could be a total content of alkaline solution with density that will negatively affect fiber-matrix bonding or voids (less strong in flexure). The compressive model also shows similar significant quadratic terms, such as X_2^2 (-2.3173) and X_7^2 (-1.5067). The flexural model's X_2^2 (-0.586) and X_7^2 (-0.3983) demonstrate a similar outcome whereby, specifically, too great an impact of high ratio and/or molarity could be diminishing the strength through an excess number of unreacted alkalis resulting in efflorescence and/or micro-cracking (and, it is also important to note here) [33, 34]. The strong interaction terms and squared terms indicate the regression is worth considering their quadratic model form, as the input/mechanical performance relationship is nonlinear across the respective mix of inputs. In short, the positive main effects show that balanced precursor content, proper activator chemistry and fiber reinforcement are beneficial aspects while the interaction and squared terms are appreciating the need to consider all of these factors in combination as their input and output relationships have the potential for negative side effects in the forms of segregation, excess porosity and/or agreement unsatisfactory fiber dispersion etc. overall, the results show how the mechanical behaviour of FRAAC is formed from complex relationships that can still be explained physically, and can also be reasonably mapped using nonlinear regression models that have undergone careful validation [35]. The quadratic models established are not only statistically reliable, but also valuable information for mix proportioning and performance enhancement of FRAAC. For instance, when designing a structural mix with a CS of 60 MPa, the proposed model helps to predict the SH molarity and dosage of fiber

needed, prior to physical testing of mixtures. The proposed models were validated using additional datasets from independent investigations (not used in the initial model training), which reported predictions with a model error of less than 5%, indicating a strong generalization ability. The proposed models can act as a decision-support tool in the optimization of binder content, activator ratios, and fiber selection in sustainable precast elements, pavement blocks, and repair mortars. Case-specific testing determined that maintaining an SS/SH ratio between 1.8 and 2.2, along with an SH molarity of 12 M, achieved the best compromise between workability and strength. These conclusions suggest that data-driven modeling could be an alternative to laboratory mix optimization and may facilitate the adoption of FRAAC as a sustainable concrete system, compared to conventional methods.

Table 3. Statistical summary of the CS model

Term	Coefficient	Estimate	SE	tStat	p-Value
Intercept	β_0	-659.48	58.379	-11.296	1.2767e-19
X_1	β_1	0.32422	0.028895	11.221	1.8660e-19
X_2	β_2	22.711	4.6331	4.9019	3.6299e-06
X_3	β_3	752.09	148.07	5.0794	1.7376e-06
X_4	β_4	0.20403	0.081388	2.5069	0.013774
X_5	β_5	-0.073295	0.038458	-1.9059	0.039509
X_6	β_6	0.12826	0.047196	2.7175	0.0077411
X_7	β_7	78.948	5.8992	13.383	4.1925e-24
X_1*X_2	β_{12}	-0.024749	0.0033473	-7.3938	4.2717e-11
X_1*X_3	β_{13}	-0.26668	0.039417	-6.7656	8.8180e-10
X_1*X_4	β_{14}	0.00042382	0.00017644	2.4021	0.018128
X_1*X_7	β_{17}	-0.010887	0.0021048	-5.1726	1.1736e-06
X_2*X_3	β_{23}	25.228	10.761	2.3444	0.021014
X_2*X_4	β_{24}	-0.089427	0.031523	-2.8368	0.0055063
X_3*X_6	β_{36}	-0.28637	0.10537	-2.7176	0.0077383
X_3*X_7	β_{37}	-103.01	9.0987	-11.322	1.1253e-19
X_1^2	β_{11}	5.9945e-05	2.4047e-05	2.4928	0.014299
X_2^2	β_{22}	-2.3173	0.22379	-10.355	1.4849e-17
X_3^2	β_{33}	595.6	118.17	5.0401	2.0475e-06
X_5^2	β_{55}	0.00038673	0.00017429	2.2189	0.028732
X_7^2	β_{77}	-1.5067	0.23702	-6.3568	6.0250e-09

Table 4. Statistical summary of the FS model

Term	Coefficient	Estimate	Standard Error (SE)	t-Statistic	p-Value
Intercept	β_0	-103.29	16.635	-6.2092	1.2225e-08
X_1	β_1	0.028411	0.00478	5.9437	4.091e-08
X_2	β_2	2.1867	0.74243	2.9454	0.0040125
X_3	β_3	121.83	39.807	3.0606	0.0028368
X_4	β_4	0.079768	0.039179	2.036	0.044397
X_5	β_5	0.073476	0.012332	5.9579	3.8366e-08
X_6	β_6	-0.00095696	0.00059043	-1.6208	0.10821
X_7	β_7	11.37	1.3809	8.2337	7.1252e-13
$X_1:X_2$	β_{12}	-0.0038518	0.00061995	-6.213	1.2012e-08
$X_1:X_7$	β_{17}	-0.001413	0.0003326	-4.2483	4.8372e-05
$X_2:X_7$	β_{27}	0.49586	0.095577	5.1881	1.1147e-06
$X_3:X_5$	β_{35}	-0.16565	0.028478	-5.817	7.2242e-08
$X_3:X_7$	β_{37}	-7.6936	2.95	-2.608	0.010501
$X_4:X_7$	β_{47}	-0.0070082	0.0031572	-2.2198	0.028694
$X_5:X_6$	β_{56}	7.8644e-05	1.9606e-05	4.0113	0.00011661
X_2^2	β_{22}	-0.58601	0.056617	-10.35	1.6902e-17
X_7^2	β_{77}	-0.39829	0.044811	-8.8881	2.6968e-14

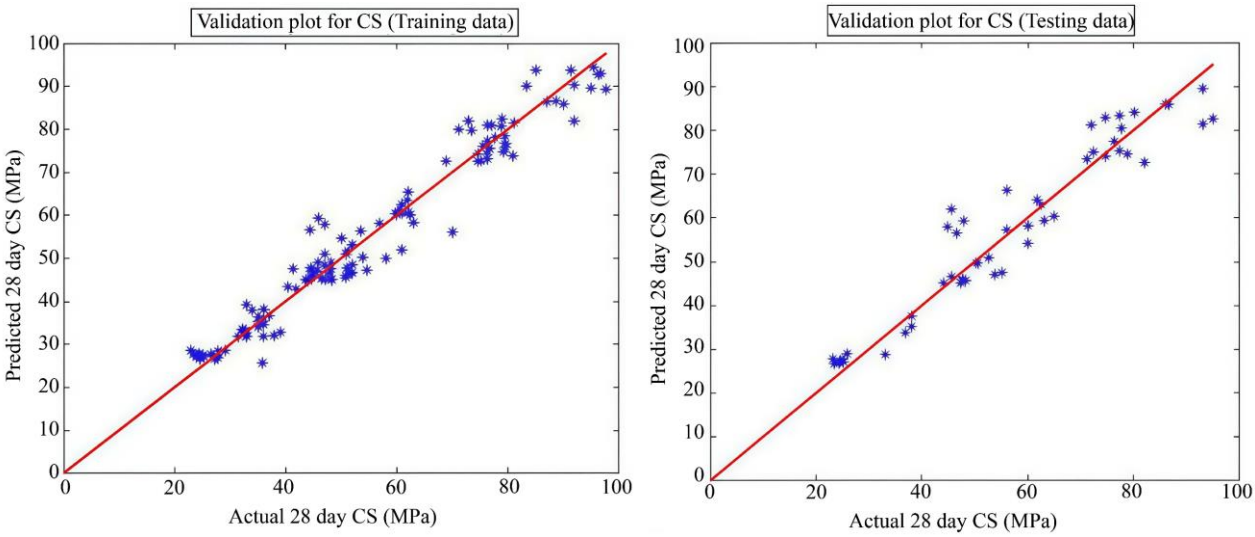

Fig. 1 Validation plots for the CS model

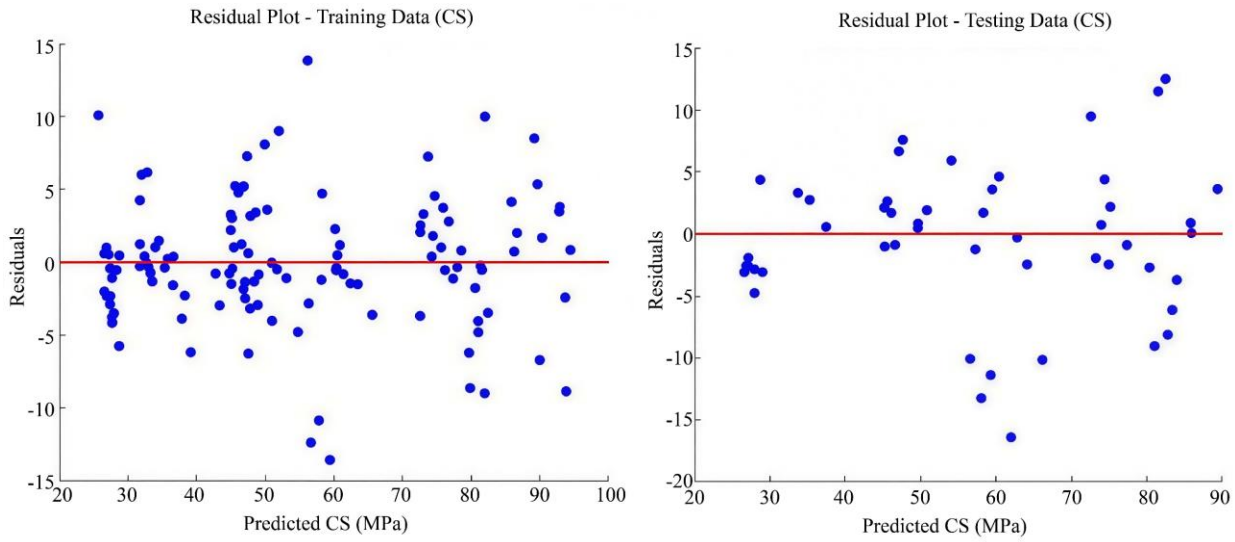

Fig. 2 Residual plots for the CS model

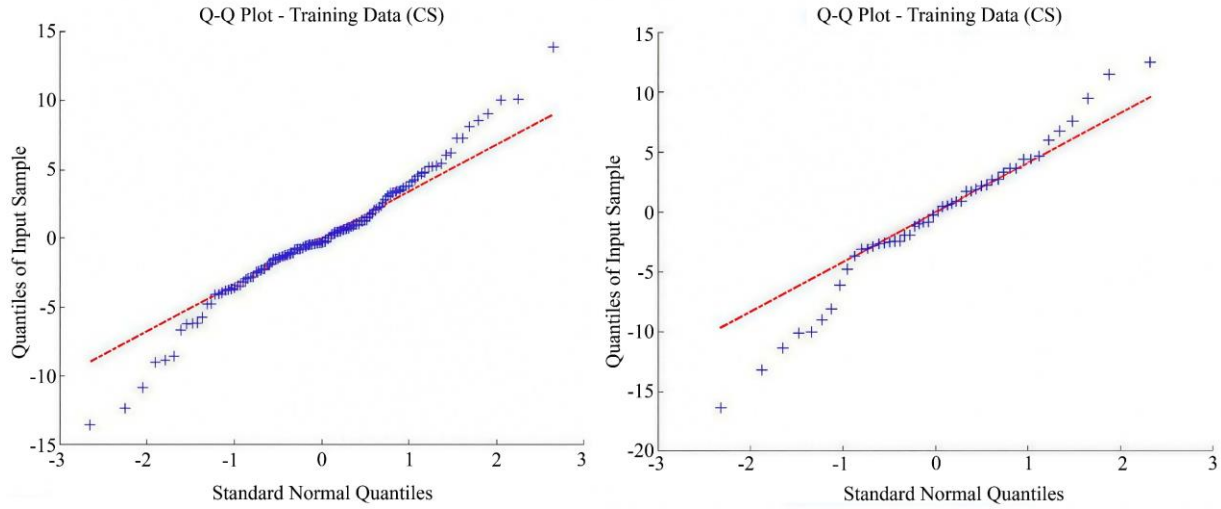

Fig. 3 Q-Q plots for the CS model

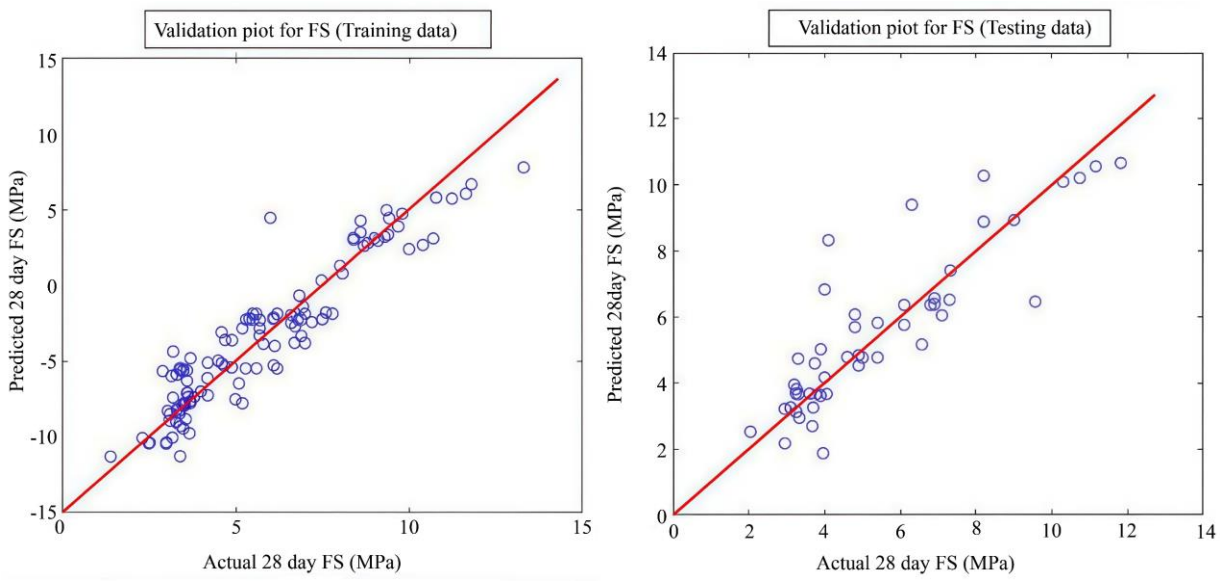

Fig. 4 Validation plots for the FS model

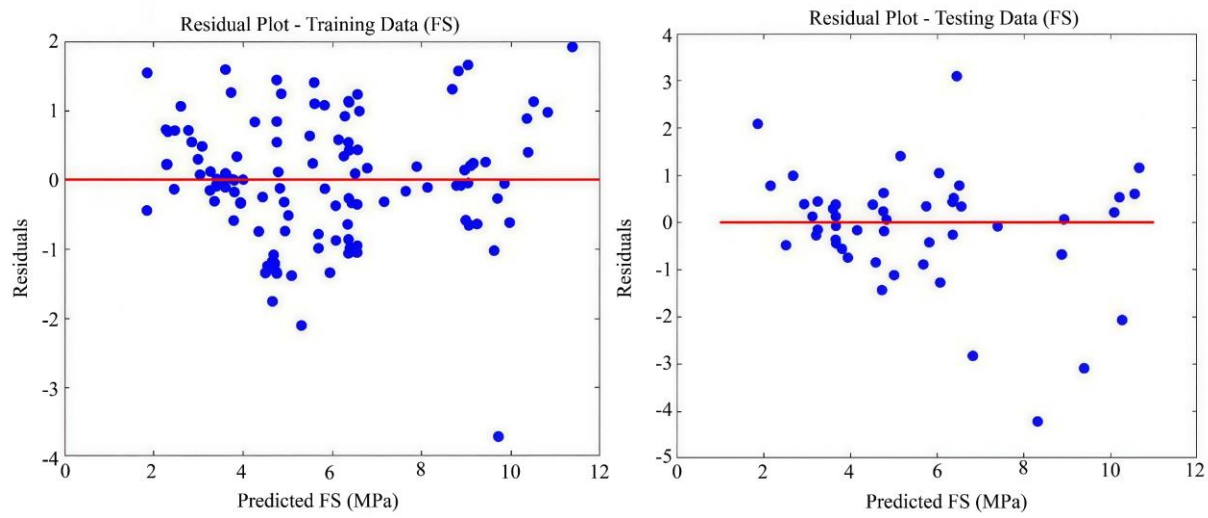

Fig. 5 Residual plots for the FS model

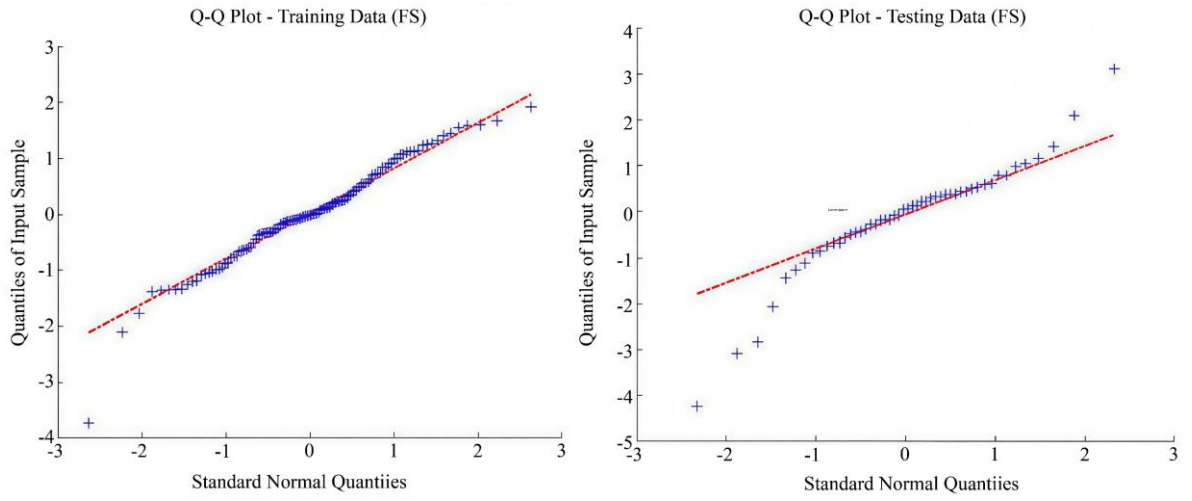

Fig. 6 Q-Q plots for the FS model

5. Conclusion

This study aimed to accurately model the mechanical behaviour of FRAAC utilising quadratic NLR modelling methods. The research explored the increasing interest and need for sustainable and high-performance alternatives to traditional concrete, and it also demonstrated how interactions between mix design and fibre properties can affect compressive and flexural strength. Relevant conclusions based on the modelling study and statistical validation can be drawn:

- The quadratic regression model yielded an R^2 of 0.93 for the training data and an R^2 of 0.96 for the testing data, meaning that the model explains over 90% of the variability in CS and has excellent predictive power.
- The RMSE for FS is 1.2008 MPa (training) and 0.8844 MPa (testing), demonstrating limited prediction error and that the model is reliable and consistent.
- The complete model R^2 for the FS function is 0.915 with an RMSE of 0.957 MPa, showing excellent performance for both training and testing datasets, as well as good generalization of the model.
- The VIF of all inputs (X_1 = 1.4711, X_5 = 1.6818) is less than the value of 5, indicating that the effect of multicollinearity is not serious, and the regression coefficients are interpretable and stable.
- The molarity of SH has a significant positive linear effect on CS (78.948), while the quadratic term (–1.5067) indicates declining returns at excessively high SH molarity.
- Q-Q plots indicate that the residuals from the models of both CS and FS are approximately normally distributed, which verifies the linear predictions and increases confidence in statistical inference.
- The residual plots for the training and testing datasets are evenly dispersed around zero with no patterns observed, which validates the generalization of the model and the absence of overfitting.

References

[1] Surajit Hore, and Amit Shiuly, "Study of Thermal Conductivity of Different Types of Alkali-Activated Concrete: A Comprehensive Review," *Environment, Development and Sustainability*, vol. 27, pp. 5525-5572, 2025. [CrossRef] [Google Scholar] [Publisher Link]

[2] Kaku Mahendra, and Mattur C. Narasimhan, "One Part Alkali-Activated Materials for Construction–A Review," *Materials Today: Proceedings*, vol. 93, pp. 182-188, 2023. [CrossRef] [Google Scholar] [Publisher Link]

[3] Huixia Wu et al., "Reusing Waste Clay Brick Powder for Low-Carbon Cement Concrete and Alkali-Activated Concrete: A Critical Review," *Journal of Cleaner Production*, vol. 449, 2024. [CrossRef] [Google Scholar] [Publisher Link]

[4] Wenlin Tu, and Mingzhong Zhang, "Multiscale Microstructure and Micromechanical Properties of Alkali-Activated Concrete: A Critical Review," *Cement and Concrete Composites*, vol. 152, 2024. [CrossRef] [Google Scholar] [Publisher Link]

[5] Isabel Pol Segura et al., "A Review: Alkali-Activated Cement and Concrete Production Technologies Available in the Industry," *Heliyon*, vol. 9, no. 5, pp. 1-24, 2023. [CrossRef] [Google Scholar] [Publisher Link]

[6] Hadi Bahmani, and Davood Mostofinejad, "Microstructural Characterization of Alkali-Activated Concrete using Waste-Derived Activators from Industrial and Agricultural Sources: A Review," *Case Studies in Construction Materials*, vol. 22, pp. 1-20, 2025. [CrossRef] [Google Scholar] [Publisher Link]

[7] Kennedy C. Onyelowe et al., "Optimizing the Utilization of Metakaolin in Pre-Cured Geopolymer Concrete using Ensemble and Symbolic Regressions," *Scientific Reports*, vol. 15, pp. 1-34, 2025. [CrossRef] [Google Scholar] [Publisher Link]

[8] Mana Alyami et al., "Hybrid Metaheuristic Optimized Random Forest Models for Predicting Compressive Strength of Alkali Activated Concrete," *Journal of Natural Fibers*, vol. 22, no. 1, pp. 1-32, 2025. [CrossRef] [Google Scholar] [Publisher Link]

[9] Zixin He et al., "Optimization of Alkali-Activated Mortar Utilizing Municipal Solid Waste Incinerator Bottom Ash and Slag: A Multi-Objective Response Surface Method Approach," *Construction and Building Materials*, vol. 458, pp. 1-18, 2025. [CrossRef] [Google Scholar] [Publisher Link]

[10] Saif Saad Mansoor et al., "Sustainable Alkali-Activated Concrete Modified with Cement Kiln Dust and Fly Ash: An Ai-Based Study," *Innovative Infrastructure Solutions*, vol. 10, 2025. [CrossRef] [Google Scholar] [Publisher Link]

[11] Alaa M. Morsy et al., "Experimental Verification for Machine-Learning Approaches in Compressive Strength Prediction of Alkali-Activated Concrete," *Journal of Structural Design and Construction Practice*, vol. 30, no. 1, 2025. [CrossRef] [Google Scholar] [Publisher Link]

[12] Yingjie Li et al., "Fresh State and Strength Performance Evaluation of Slag-Based Alkali-Activated Concrete using Soft-Computing Methods," *Materials Today Communications*, vol. 38, 2024. [CrossRef] [Google Scholar] [Publisher Link]

[13] Mo Zhang et al., "Effect of Composition and Curing on Alkali Activated Fly Ash-Slag Binders: Machine Learning Prediction with a Random Forest-Genetic Algorithm Hybrid Model," *Construction and Building Materials*, vol. 366, 2023. [CrossRef] [Google Scholar] [Publisher Link]

[14] Torkan Shafighfard et al., "Machine-Learning Methods for Estimating Compressive Strength of High-Performance Alkali-Activated Concrete," *Engineering Applications of Artificial Intelligence*, vol. 136, 2024. [CrossRef] [Google Scholar] [Publisher Link]

[15] Jian Gao et al., "R-Squared (R^2)–How Much Variation is Explained?," *Research Methods in Medicine & Health Sciences*, vol. 5, no. 4, pp. 104-109, 2023. [CrossRef] [Google Scholar] [Publisher Link]

[16] Meysam Alizamir et al., "An Interpretable XGBoost-SHAP Machine Learning Model for Reliable Prediction of Mechanical Properties in Waste Foundry Sand-Based Eco-Friendly Concrete," *Results in Engineering*, vol. 25, pp. 1-29, 2025. [CrossRef] [Google Scholar] [Publisher Link]

[17] Uzoma Ibe Iro et al., "Optimization of Cassava Peel Ash Concrete using Central Composite Design Method," *Scientific Reports*, vol. 14, pp. 1-23, 2024. [CrossRef] [Google Scholar] [Publisher Link]

[18] Felipe Guíñez et al., "Effect of Mix Dosage on Rubberized Concrete Mechanical Performance: A Multivariable Prediction Model towards Design Provisions," *Journal of Building Engineering*, vol. 90, 2024. [CrossRef] [Google Scholar] [Publisher Link]

[19] Hemn Unis Ahmed, Ahmed S. Mohammed, and Azad A. Mohammed, "Multivariable Models Including Artificial Neural Network and M5P-Tree to Forecast the Stress at the Failure of Alkali-Activated Concrete at Ambient Curing Condition and Various Mixture Proportions," *Neural Computing and Applications*, vol. 34, pp. 17853-17876, 2022. [CrossRef] [Google Scholar] [Publisher Link]

[20] Y.S.N. Kishore et al., "Statistical Analysis of Sustainable Geopolymer Concrete," *Materials Today: Proceedings*, vol. 61, no. 2, pp. 212-223, 2022. [CrossRef] [Google Scholar] [Publisher Link]

[21] David Conciatori et al., "Statistical Analysis of Concrete Transport Properties," *Materials and Structures*, vol. 47, pp. 89-103, 2014. [CrossRef] [Google Scholar] [Publisher Link]

[22] Huibert Jilles Bezemer, and Mladena Luković, "Early-Age and Long-Term Deformations in Reinforced Slag-Based Alkali Activated Concrete," *Construction and Building Materials*, vol. 476, pp. 1-12, 2025. [CrossRef] [Google Scholar] [Publisher Link]

[23] Biswajit Majhi, Rohit Ranjan, and Subhajit Mondal, "Multi Response Optimization of Recycled Aggregate Based Alkali-Activated Concrete using Taguchi-Grey Relational Analysis Method," *Construction and Building Materials*, vol. 441, 2024. [CrossRef] [Google Scholar] [Publisher Link]

[24] Osama A. Mohamed et al., "Effect of Activator Concentration on Setting Time, Workability and Compressive Strength of Sustainable Concrete with Alkali-Activated Slag Binder," *Materials Today: Proceedings*, 2024. [CrossRef] [Google Scholar] [Publisher Link]

[25] Husam Alsarhan, and Amin Al-Fakih, "Performance and Sustainability of Industrial By-Products-Based Alkali-Activated Concrete: A Review," *Multiscale and Multidisciplinary Modeling, Experiments and Design*, vol. 8, 2025. [CrossRef] [Google Scholar] [Publisher Link]

[26] Feng Wu et al., "Size Effect in the Mechanical Characteristics of Steel Fiber Reinforced Alkali-Activated Slag/Fly Ash-Based Concrete," *Construction and Building Materials*, vol. 443, 2024. [CrossRef] [Google Scholar] [Publisher Link]

[27] Amr Hassan et al., "Effect of Hybrid Polypropylene Fibers on Mechanical and Shrinkage Behavior of Alkali-Activated Slag Concrete," *Construction and Building Materials*, vol. 411, 2024. [CrossRef] [Google Scholar] [Publisher Link]

[28] Nailia Rakhimova, and Caijun Shi, "Upcycling of Concrete Wastes as Precursors in Alkali-Activated Materials: A Review," *Construction and Building Materials*, vol. 436, 2024. [CrossRef] [Google Scholar] [Publisher Link]

[29] Shashwati Soumya Pradhan et al., "Development of Sustainable Slag-Based Alkali-Activated Concrete Incorporating Fly Ash at Ambient Curing Conditions," *Energy, Ecology and Environment*, vol. 9, pp. 563-577, 2024. [CrossRef] [Google Scholar] [Publisher Link]

[30] Mugahed Amran et al., "Fiber-Reinforced Alkali-Activated Concrete: A Review," *Journal of Building Engineering*, vol. 45, 2022. [CrossRef] [Google Scholar] [Publisher Link]

[31] Laura Rossi, Ravi A. Patel, and Frank Dehn, "New Analytical Models to Predict the Mechanical Performance of Steel Fiber-Reinforced Alkali-Activated Concrete," *Structural Concrete*, vol. 26, no. 1, pp. 236-247, 2025. [CrossRef] [Google Scholar] [Publisher Link]

[32] Siyuan Zhang et al., "The Stress-Strain Behavior, Durability, and Equilibrium Analysis of Copper-Coated Steel Fibers Reinforced Alkali-Activated Concrete," *Construction and Building Materials*, vol. 462, 2025. [CrossRef] [Google Scholar] [Publisher Link]

[33] Pathi Janardhan, R. Venkata Krishnaiah, and K.V.B. Raju, "Experimental Study on the Performance of Strength and Sorptivity of Fiber Reinforced Alkali Activated Geopolymer Concrete," *Materials Today: Proceedings*, 2024. [CrossRef] [Google Scholar] [Publisher Link]

[34] Tejaswini G. Panse et al., "Predictive Performance of Nano-Alumina and Zeolite-Based High-Performance Nano-Engineered Concrete: Integrative Application of Quantum Computing and Machine Learning with Optimization Techniques," *Quantum Machine Intelligence*, vol. 7, 2025. [CrossRef] [Google Scholar] [Publisher Link]

[35] Ravinder Kampa, and S. Venkateswara Rao, "Influence of Fiber Reinforcement on the Strength and Durability of High Strength Geopolymer Concrete with Multi Component Precursors," *Engineering Research Express*, vol. 7, pp. 1-16, 2025. [CrossRef] [Google Scholar] [Publisher Link]

[36] Houcine Bentegri et al., "Assessment of Compressive Strength of Eco-Concrete Reinforced using Machine Learning Tools," *Scientific Reports*, vol. 15, pp. 1-24, 2025. [CrossRef] [Google Scholar] [Publisher Link]